ChemMedChem

ResearchArticle
doi.org/10.1002/cmdc.202200021

Chemistry Europe
European Chemical Societies Publishing

www.chemmedchem.org

New Insight into Dearomatization and Decarbonylation of Antitubercular 4*H*-Benzo[*e*][1,3]thiazinones: Stable 5*H*- and 7*H*-Benzo[*e*][1,3]thiazines

Adrian Richter,[a] Rüdiger W. Seidel,[a] Jürgen Graf,[b] Richard Goddard,[c] Christoph Lehmann,[a] Tom Schlegel,[a] Nour Khater,[a] and Peter Imming*[a]

Dedicated to Professor Wolfgang Seidel on the occasion of his 90th birthday.

8-Nitro-4*H*-benzo[*e*][1,3]thiazinones (BTZs) are potent *in vitro* antimycobacterial agents. New chemical transformations, *viz.* dearomatization and decarbonylation, of two BTZs and their influence on the compounds' antimycobacterial properties are described. Reactions of 8-nitro-2-(piperidin-1-yl)-6-(trifluoromethyl)-4*H*-benzo[*e*][1,3]thiazin-4-one and the clinical drug candidate BTZ043 with the Grignard reagent CH_3MgBr afford the corresponding dearomatized stable 4,5-dimethyl-5*H*- and 4,7-dimethyl-7*H*-benzo[*e*][1,3]thiazines. These methine compounds are structurally characterized by X-ray crystallography for the first time. Reduction of the BTZ carbonyl group, leading to the corresponding markedly non-planar 4*H*-benzo[e][1,3]thiazine systems, is achieved using the reducing agent $(CH_3)_2S{\cdot}BH_3$. Double methylation with dearomatization and decarbonylation renders the two BTZs studied inactive against *Mycobacterium tuberculosis* and *Mycobacterium smegmatis*, as proven by *in vitro* growth inhibition assays.

Introduction

8-Nitro-4*H*-benzo[*e*][1,3]thiazinones (BTZs) **1a** and **1b** (BTZ043) are known as potent antitubercular agents (Scheme 1).[1] After entering the catalytic site of decaprenylphosphoryl-β-D-ribose 2′-epimerase (DprE1), a mycobacterial enzyme crucial for cell wall synthesis, the 8-nitro group is reduced to a nitroso group, which covalently binds to a cysteine residue. BTZs inhibit DprE1 at μM to nM minimum inhibitory concentrations (MICs). High target- and species-specificity renders BTZs promising antitubercular drug candidates. Compound **1b** and macozinone (PBTZ169)[2] have reached clinical trials.[3] However, stability problems, especially metabolic reduction of the nitro group and BTZ core, and the relatively high dosage of 300–600 mg/day in clinical studies[2] in spite of the very high *in vitro* activity motivate further research on this compound class.

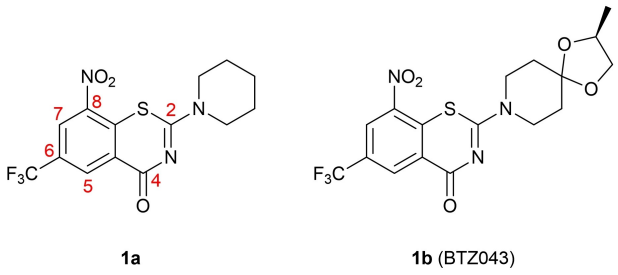

Scheme 1. Chemical diagrams of the antitubercular BTZs **1a** and **1b** (BTZ043).

BTZs feature various reactive centres for nucleophilic attack. Thiols and other nucleophiles were shown to attack C7 of the 4*H*-benzo[e][1,3]thiazinone system, resulting in non-enzymatic reduction of the 8-nitro group *via* a von Richter rearrangement.[4] We did, however, not observe nucleophilic attack at C7 when incubating BTZs with DprE1.[5]

Recently, we showed by X-ray crystallography that treatment of **1a** and **1b** with moist 3-chloroperbenzoic acid unexpectedly led to the corresponding benzo[*d*]isothiazol-3(2*H*)-ones and their 1-oxides,[6] instead of the anticipated corresponding BTZ sulfones and sulfoxides,[7] presumably involving nucleophilic addition of water at C2. In their search for the structure of a human plasma metabolite of **1b**, Kloss *et al.* found that treatment of the compound with the reducing agent $NaBH_4$ yielded Meisenheimer complexes, which were also encountered in *ex vivo* studies.[8] Furthermore, they reported that reaction with the Grignard reagent CH_3MgBr resulted in

[a] Dr. A. Richter, Dr. R. W. Seidel, C. Lehmann, T. Schlegel, N. Khater, Prof. Dr. P. Imming
Institut für Pharmazie
Martin-Luther-Universität Halle-Wittenberg
Wolfgang-Langenbeck-Str. 4
06120 Halle (Saale) (Germany)
E-mail: peter.imming@pharmazie.uni-halle.de
[b] Dr. J. Graf
Incoatec GmbH
Max-Planck-Str. 2
21502 Geesthacht (Germany)
[c] Dr. R. Goddard
Max-Planck-Institut für Kohlenforschung
Kaiser-Wilhelm-Platz 1
45470 Mülheim an der Ruhr (Germany)

Supporting information for this article is available on the WWW under https://doi.org/10.1002/cmdc.202200021

the 5- and 7-monomethyl derivatives of **1 b**. A very recent study proved the importance of electron-deficient (nitro-)aromatic pharmacophores in covalent DprE1 inhibitors, which showed comparable reactivity towards $NaBH_4$.[9]

Identification of possible reaction pathways of BTZs is important for understanding and optimization of absorption, distribution, metabolism and excretion (ADME) characteristics and of particular interest with regard to the ongoing investigation of this compound class in medicinal chemistry,[10] pharmaceutics[11] and clinical development.[3a]

We have now (re)investigated reactions of BTZs **1 a** and **1 b** with CH_3MgBr and the reducing agent $(CH_3)_2S\cdot BH_3$. Treatment with CH_3MgBr and workup afforded doubly methylated benzothiazinone scaffolds, resulting in stable 5*H*- and 7*H*-benzo[*e*][1,3]-thiazines. Reactions of **1 a** and **1 b** with $(CH_3)_2S\cdot BH_3$ resulted in 8-amino- and 8-nitro-6-(trifluoromethyl)-4*H*-benzo[*e*][1,3]-thiazines, demonstrating the possibility of selectively reducing the carbonyl carbon atom C4 in BTZs.

Results and Discussion

Reaction of BTZs 1 a and 1 b with CH_3MgBr

BTZs **1 a** and **1 b** were reacted with two equivalents of CH_3MgBr in THF/Et_2O (Scheme 2). Upon quenching with water, the color of the reaction mixture immediately turned red. Nucleophilic additions to C5 and C7 of the BTZ scaffold occurred, which presumably led to intermediate thiazin-4-ol derivatives **2**, **4**, **6** and **8** (not isolated) after hydrolysis. Subsequent elimination of water afforded the dimethyl-5*H*- and 7*H*-benzo[*e*][1,3]thiazine isomers **3** and **5**, which were extracted from the aqueous mixture with ethyl acetate and separated by flash chromatography. Acidification of the remaining aqueous phase (pH 2–3) with dilute hydrochloric acid led to the 5- and 7-methyl-BTZs **7** and **9** as mixtures of structural isomers, as described by Kloss *et al.*,[8] which were likewise separated by flash chromatography. An acidic reaction medium appeared to be essential for reoxidation of the BTZ system by air. Compounds **3**, **5**, **7** and **9** were identified by NMR spectroscopy and HRMS and in part by X-ray crystallography. In contrast to BTZs, the 5*H*- and 7*H*-benzo[*e*][1,3]thiazines **3** and **5** exhibited a red color with an intense absorption band centered at around 500 nm in methanol (Figure S1 in the Supporting Information).

The yields for the individual isolated reaction products (**3**, **5**, **7** and **9**) after treatment of **1** with CH_3MgBr are within 2–11 %. These low yields are partly due to the fact that four different compounds were isolated from one reaction. If the yields of the individual products are added up, approx. 25 % of **1** is converted to the products studied. Furthermore, demanding chromatographic separations of the isomeric compounds lowered the yields, and we assume that **1** in part decomposes when treated with CH_3MgBr.

Figure 1 shows the ^1H NMR spectra of **3 a**, **5 a**, **7 a**, **9 a** and the parent BTZ **1 a**. Those of **3 b**, **5 b**, **7 b**, **9 b** and the parent **1 b** are depicted in the Supporting Information (Figure S2). Monomethylation of the benzene moiety in **7 a** and **9 a** caused a slight upfield shift of the remaining aromatic signal. In the 5*H*- and 7*H*-benzo[*e*][1,3]thiazines **3 a** and **5 a**, the resonance signals assigned to the methine hydrogen atoms at the sp^2 carbon

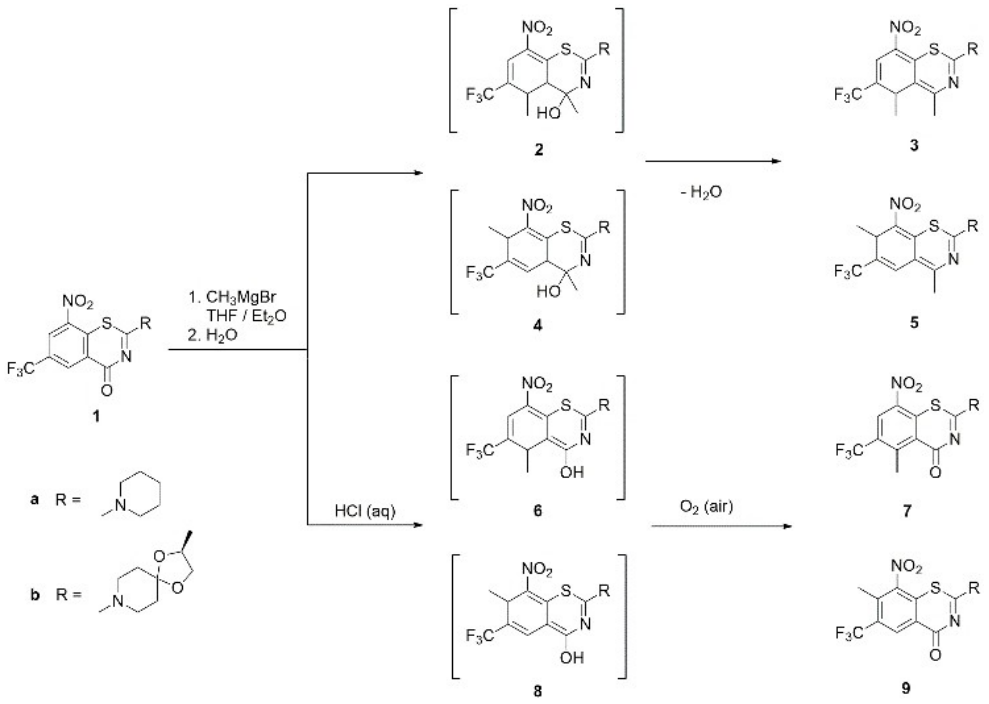

Scheme 2. Reaction products after treatment of BTZs **1 a** and **1 b** with the Grignard reagent CH_3MgBr, subsequent hydrolysis and dehydration (**3** and **5**) or air oxidation (**7** and **9**). Compounds **2**, **4**, **6** and **8** were not isolated.

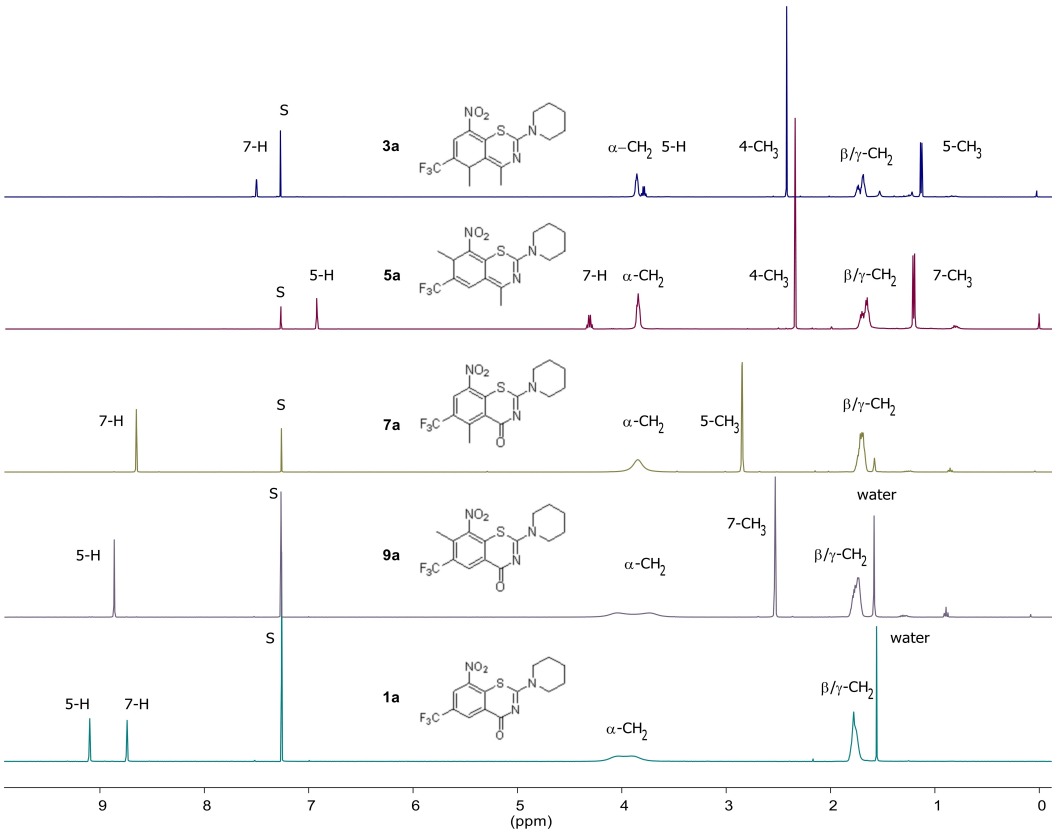

Figure 1. ^{1}H NMR spectra (400 MHz, $CDCl_3$) of the 5*H*- and 7*H*-benzo[*e*][1,3]thiazines **3a** and **5a**, the monomethyl BTZs **7a** and **9a** and the parent BTZ **1a**. S denotes the residual solvent signal.

atoms C7 and C5, occurred at higher field than the corresponding aromatic signals in the BTZs **1a**, **7a** and **9a**. The hydrogen atoms at the sp^3 carbon atoms C5 in **3a** and C7 in **5a** gave rise to quartet signals at 4.34 and 3.81 ppm. Whereas the positions of the signals assigned to the α-H atoms of the piperidine ring remained nearly unaffected by methylation of the BTZ moiety, these signals are significantly sharper in the 5*H*- and 7*H*-benzo[*e*][1,3]thiazines **3a** and **5a** than in the BTZs **1a**, **7a** and **9a** (Figure 1). This indicates restricted rotation of the piperidine ring about the C2–$N_{piperidine}$ bond in **3a** and **5a** in $CDCl_3$ solution at room temperature.

Slow diffusion of heptane into solutions of **3a** and **5a** in chloroform afforded small red needles of the compounds. X-ray crystallography unambiguously revealed the molecular structures (Figure 2). To the best of our knowledge and based on a search of the Cambridge Structural Database (CSD),[12] these are the first structural characterizations of 5*H*- and 7*H*-benzo[*e*]-1,3-thiazine heterocyclic systems. A chirality centre resulted from nucleophilic addition of the methyl group at C5 and C7 of the benzothiazine scaffold in **3** and **5**. The methylations are not stereoselective. Thus, racemates were formed. This is reflected in the centrosymmetric crystal structures of **3a** and **5a**, which comprise both enantiomers. The fused bicyclic systems are not planar. C5 is located 0.293(3) Å in **3a** and 0.207(6) Å in **5a** above the mean plane through the nearly planar six-membered 1,3-thiazine ring (r.m.s. deviation 0.0365 Å in **3a** and 0.0225 Å in **5a**), whereas C7 lies 0.420(3) Å and 0.377(7) Å below this plane in **3a** and **5a**, respectively. Table 1 compares selected bond lengths of the dearomatized benzothiazine system for both structures. The C–S bond lengths are consistent with Csp^2–S single bond character, and the C2–N3 bond lengths are as expected for a Csp^2=N double bond. The C4–C4A, C6–C7 (in **3a**) or C5–C6 (in **5a**) and C8–C8A bond lengths indicate Csp^2=Csp^2 double bond character.[13] The appended piperidine ring adopts a low energy chair conformation in both **3a** and **5a** with some minor deviations from ideal tetrahedral angles, which can be attributed to the planar structure at N1.

For enantiopure **1b**, non-stereoselective double methylation resulted in a mixture of *RS* and *SS* diastereomers in **3b**

Table 1. Selected bond lengths (Å) for **3a**, **5a** and **10a**.

	3a	5a	10a
C2–S1	1.7581(18)	1.775(4)	1.8095(13)
C8A–S1	1.7546(18)	1.752(4)	1.7635(13)
C2–N3	1.329(2)	1.321(5)	1.2748(17)
C4–N3	1.339(2)	1.344(5)	1.4635(16)
C4–C4A	1.407(2)	1.395(5)	1.5007(17)
C4A–C5	1.528(2)	1.454(5)	1.3890(18)
C5–C6	1.508(3)	1.332(6)	1.3927(18)
C6–C7	1.331(3)	1.508(5)	1.3851(18)
C7–C8	1.441(3)	1.515(5)	1.3883(18)
C8–C8A	1.414(2)	1.393(5)	1.3997(17)

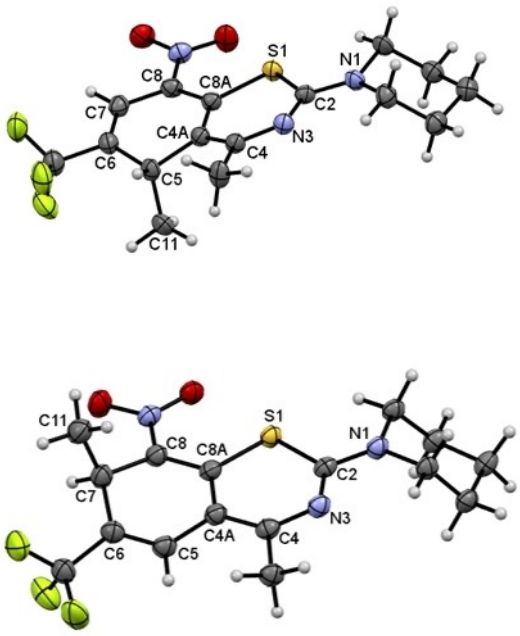

Figure 2. Molecular structures of **3 a** (top) and **5 a** (bottom) in the crystal, showing the *R* enantiomer in both cases. Displacement ellipsoids are drawn at the 50% probability level. Hydrogen atoms are represented by small spheres of arbitrary radius. The minor part of the rotationally disordered trifluoromethyl group (ca. 3%) in **5 a** is omitted clarity (see Figure S3 in the Supporting Information). Colour scheme: C grey, H white, N blue, O red, S yellow.

and **5 b**. We should note that the diastereomers of **3 b** and **5 b** could neither be distinguished by room temperature ^{1}H and ^{13}C NMR spectroscopy, routine HPLC analysis, nor be separated by flash chromatography. This is likely due to the high degree of similarity in the molecular structures. Compound **3 b** was structurally characterized by X-ray crystallography. The asymmetric unit comprises four molecules (Sohncke space group *P*1; *Z*, *Z*′ = 4).[14] There are two pairs of *RS* and *SS* diastereomers, each related by a *pseudo* centre of symmetry. The Platon/ADDSYM routine calculates 95% fit for the *pseudo* symmetry.[15] The absolute structure assignment was inferred from the known *S* configuration of the methyl-dioxolan group in the starting material **1 b** (Scheme 1) and was verified by a Flack *x* parameter close to zero.[16] Figure 3 depicts the *pseudo* centrosymmetric arrangement of unique molecules 1 (*RS* configuration) and 2 (*SS* configuration) in the crystal. A displacement ellipsoid plot for molecules 3 and 4 can be found in the Supporting Information (Figure S4). The crystal of **3 b** is thus a co-crystal of diastereomers, indicating that the diastereomers of **3 b** are also not easily if at all separable by crystallization. A similar situation was previously encountered in the crystal structure of the corresponding benzisothiazolinone 1-oxide derived from **1 b**, where oxidation led to a second centre of chirality at the sulfur atom.[6] Structural parameters of the 5*H*-benzo[*e*]-1,3-thiazine heterocyclic system in **3 b** are similar to those in **3 a**. The piperidine ring exhibits a chair conformation in all four distinct molecules. In molecule 4, positional disorder of the methyl-dioxolan group, resulting from an approximate 180° rotation of the side chain

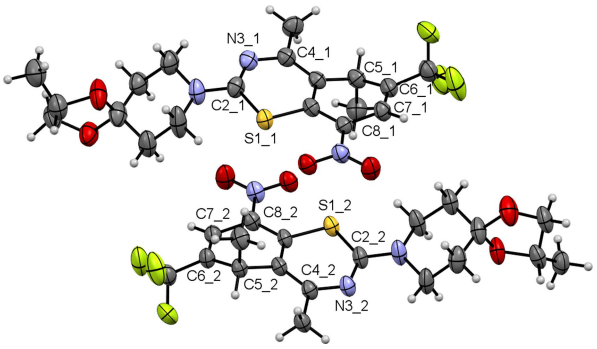

Figure 3. Part of the asymmetric unit of **3 b**. Displacement ellipsoids are drawn at the 50% probability level. Hydrogen atoms are represented by small spheres of arbitrary radius. For the sake of clarity only unique molecules 1 and 2 (as indicated by the number after the underscore) are depicted (for molecules 3 and 4, see Supporting information). Colour scheme: C grey, H white, N blue, O red, S yellow.

about the C2–$N_{piperidine}$ formal single bond, is encountered (see Figure S4 in the Supporting Information).

The structure of **7 b** was likewise confirmed by X-ray crystallography (Figure 4). Compound **7 b** crystallizes with two diastereomeric conformers in the asymmetric unit, which are related by *pseudo* inversion symmetry (96% fit, as calculated with Platon/ADDSYM[15]). An approximate 180° rotation about the $C2_{BTZ}$–$N_{piperidine}$ formal single bond interconverts the two diastereomeric conformers. The six-membered ring of the 1,3-thiazinone moiety exhibits a slight boat shape and, as expected, the piperidine ring adopts a low-energy chair conformation. The plane of the nitro group and the mean plane of the benzene ring are inclined at 18.10° in molecule 1 and 17.95° in molecule 2. The structure of **7 b** is isomorphous with that of the parent compound **1 b**, which has been described in detail elsewhere.[17]

In order to study the influence of methylation and dearomatization of the benzothiazinone scaffold on antimycobacterial properties, mycobacterial growth inhibition assays

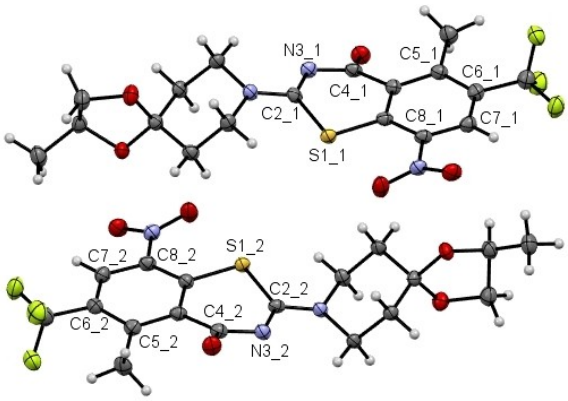

Figure 4. Displacement ellipsoid plot of **7 b** (50% probability level). Hydrogen atoms are represented by small spheres of arbitrary radius. The number after the underscore indicates the crystallographically unique molecules 1 and 2. Colour scheme: C grey, H white, N blue, O red, S yellow.

were performed as summarized in Table 2. Against *Mycobacterium tuberculosis* H_{37}Rv, we found higher MIC_{90} values *in vitro* for the monomethyl BTZs **7a** and **9a** than for the parent compound **1a**. Against *Mycobacterium smegmatis* mc^2 155, a fast-growing mycobacterium and model for the pathogen *M. tuberculosis*,[18] **7a** and **9a** were found to be inactive. The parent **1a** inhibits growth of *M. smegmatis* mc^2 155. Consistent with literature data,[19] the monomethyl BTZs **7b** and **9b**, derived from **1b** (BTZ043), were found to be potent antitubercular agents, albeit likewise less active than the parent **1b**. In contrast to **7a** and **9a**, **7b** and **9b** still display activity against *M. smegmatis* mc^2. This suggests that the side chain appended to C2 of the benzothiazinone scaffold appears to have a crucial bearing on the *in vitro* antimycobacterial activity also for the monomethyl–BTZs. For both **1a** and **1b** it was observed that in particular the introduction of a methyl group in the 5-position of the benzothiazinone scaffold decreases *in vitro* activity against both mycobacterial strains.

The 5*H*- and 7*H*-benzo[*e*][1,3]thiazines **3** and **5** were subjected to *in vitro* activity testing against *M. smegmatis* mc^2 155. We found a low level of antimycobacterial activity for **5b** (MIC_{90} 25 μM), whereas **3a** (>100 μM), **3b** (100 μM) and **5a** (>100 μM) were found be inactive. It is interesting to note that in the crystal structure of the *M. tuberculosis* DprE1 in complex with PBTZ169 (PDB code: 4NCR, resolution 1.88 Å) a water molecule links the BTZ carbonyl oxygen atom in the 4-position to a backbone carbonyl oxygen atom of a leucine moiety through hydrogen bonding.[20] Similarly, in the crystal structures of the *M. tuberculosis* DprE1 in complex with related BTZs, a hydrogen-bonded water molecule joins the BTZ carbonyl oxygen atom to the backbone carbonyl atom of a tyrosine moiety.[5] The absence of the carbonyl group at C4 in **3** and **5** as hydrogen bond acceptor thus likely contributes to the considerably lower antimycobacterial *in vitro* activity compared with the parent BTZs **1a** and **1b**.

Table 2. *In vitro* activity (MIC_{90} in μM) of the compounds studied against *M. smegmatis* mc^2 155 and *M. tuberculosis* H37Rv.

	M. smegmatis mc^2 155	*M. tuberculosis* H37Rv
1a	12.5	0.6
3a	>100	>100
5a	>100	>100
7a	>100	16.8
9a	>100	8.4
1b (BTZ043)	0.01	0.007
3b	100	– [a]
5b	25	– [a]
7b	5	1.1 [b]
9b	0.3	0.02 [b]
10a	>100	– [a]
11a	>100	– [a]
10b	<0.39	– [a]
11b	>100	– [a]

[a] Not determined. [b] Data taken from.[19]

Reaction of BTZs 1a and 1b with $(CH_3)_2S\cdot BH_3$

Treatment of BTZs **1a** and **1b** with the reducing agent $(CH_3)_2S\cdot BH_3$ in THF[21] and subsequent aqueous workup surprisingly resulted in selective reduction of the BTZ carbonyl group in 4-position to a methylene group with the 8-nitro benzo[*e*][1,3]thiazines **10** as major products (Scheme 3). The 8-nitro group partially underwent reduction under these reaction conditions affording the corresponding benzo[*e*][1,3]thiazine-8-amines **11** as minor products, which were separated by flash chromatography. Compounds **10** and **11** were characterized by ^{1}H and ^{13}C NMR spectroscopy and HRMS. In addition, the structure of **10a** was proven by X-ray crystallography (Figure 5). Selected bond lengths are included in Table 1. As observed previously for two rare examples of structurally characterized benzo[*e*][1,3]thiazines,[22] the heterocyclic benzothiazine system is distinctly non-planar as a result of a marked boat shape of the 1,3-thiazine ring with C2 and N3 being displaced from the mean plane through the fused benzene ring by 1.023(2) and 0.956(2) Å, respectively. The nitro group is tilted out of the benzene ring mean plane by 22.1(1)°.

The antimycobacterial activity of the decarbonylated BTZs **10** and **11** was evaluated *in vitro* against *M. smegmatis* mc^2 155 (Table 2). No growth inhibition was observed for **10a** up to a concentration of 100 μM despite the presence of the 8-nitro group necessary for covalent binding to DprE1. This observation confirmed the assumption that the 4-carbonyl group as hydrogen bonding acceptor site is also essential for efficient inhibition of DprE1 (*vide supra*). For **10b**, however, no bacterial growth of *M. smegmatis* up to a concentration of 0.39 μM was

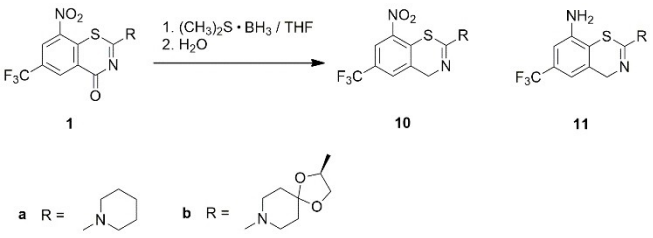

Scheme 3. Reaction products after treatment of BTZs **1a** and **1b** with the reducing agent $(CH_3)_2S\cdot BH_3$ and subsequent hydrolysis.

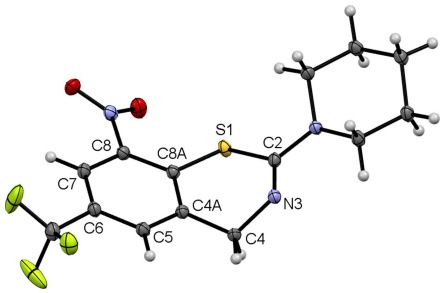

Figure 5. Molecular structure of **10a** in the crystal. Displacement ellipsoids are drawn at the 50% probability level. Hydrogen atoms are represented by small spheres of arbitrary radius. Colour scheme: C grey, H white, N blue, O red, S yellow.

observed under the same conditions. We ascribe this observation to trace reoxidation of **10b** to the parent BTZ **1b**, which was also noticeable in the ^{1}H NMR spectrum (Figure S5 in the Supporting Information). One might expect the same for **10a**, but the activity of the parent BTZ **1a** against *M. smegmatis* is some orders of magnitude lower than that of **1b** . Thus, trace amounts of **10a** could remain undetected in the *in vitro* assay used. Compounds **11a** and **11b** showed no activity against *M. smegmatis*. Apart from the absence of the 4-carbonyl group as in **10a** and **10b**, **11a** and **11b** also lack the 8-nitro group crucial for covalent binding to DprE1. Loss of antimycobacterial activity was found previously for BTZ-8-amines, as the amino group is not activated to the reactive nitroso group by the enzyme.[5,20,23]

Conclusions

The present study provides insight into the reactivity of the carbonyl group in 4-position of the BTZ scaffold of the two antitubercular 8-nitro BTZs **1a** and **1b** (BTZ043). Reaction with the Grignard reagent CH_3MgBr and the reducing agent $(CH_3)S\cdot BH_3$ reveals previously unobserved reactivity of BTZs. It has been shown that nucleophilic attack not only occurs at the electron-deficient benzene ring but also at the carbonyl carbon atom of the thiazinone ring. Treatment with CH_3MgBr afforded methylated and/or dearomatized BTZ derivatives **3**, **5**, **7** and **9**. Decarbonylation to the 4-methylene derivatives in part with concomitant reduction of the 8-nitro group was observed when the BTZs were reacted with $(CH_3)_2S\cdot BH_3$. The reductive chemical transformations encountered indicate possible points of attack for BTZs during drug metabolism. Consistent with previous findings, methyl–BTZs **7** and **9** remain active against mycobacteria *in vitro*, whereas dearomatization of BTZs **1** to **3** and **5** and decarbonylation to **10** renders these derivatives inactive against *M. tuberculosis* and *M. smegmatis*. In line with known structures of DprE1–BTZ complexes, this supports the view that the BTZ 4-carbonyl group is a hydrogen bond acceptor crucial for effective inhibition of the mycobacterial enzyme DprE1. Concomitantly, the carbonyl group also increases the electrophilicity of C-8 and the ease of reduction of the nitro group, again supporting the molecular mechanism leading to activity.

Experimental Section

Experimental procedures for the syntheses, NMR spectroscopic and HRMS characterizations, HPLC analyses (Figures S5–S53) and *in vitro* antimycobacterial testing of the compounds studied can be found in the Supporting Information.

X-ray crystallography

Details of the X-ray intensity data collections and crystal structure refinements can be found in the Supporting Information. CCDC 2126176-2126180 contain the supplementary crystallographic data for this paper. These data can be obtained free of charge from The Cambridge Crystallographic Data Centre via www.ccdc.cam.ac.uk/structures.

Crystal data for **3a** (CCDC 2126176): $C_{16}H_{18}F_3N_3O_2S$, $M_r = 373.39$, $T = 100(2)$ K, $\lambda = 0.71073$ Å, orthorhombic, space group *Pccn*, $a = 11.5451(6)$, $b = 16.7979(9)$, $c = 16.972(1)$ Å, $V = 3291.4(3)$ Å^3, $Z = 8$, $\rho_{calc} = 1.507$ mg m^{-3}, $\mu = 0.244$ mm^{-1}, $F(000) = 1552$, crystal size $0.06\times0.02\times0.01$ mm, θ range $= 2.14$–$33.23°$, reflections collected/unique $= 115254/6310$, ($R_{int} = 0.1258$), 228 parameters, $S = 1.011$, $R1[I > 2\sigma(I)] = 0.0542$, $wR2 = 0.1420$, $\Delta\rho_{max}$, $\Delta\rho_{min} = 0.27$, -0.46 eÅ^{-3}.

Crystal data for **3b** (CCDC 2126177): $C_{19}H_{22}F_3N_3O_4S$, $M_r = 445.45$, $T = 100(2)$ K, $\lambda = 1.54178$ Å, triclinic, space group *P*1, $a = 12.8795(16)$, $b = 13.3094(16)$, $c = 14.9933(19)$ Å, $\alpha = 99.359(6)$, $\beta = 106.571(5)$, $\gamma = 118.865(5)°$, $V = 2014.5(4)$ Å^3, $Z = 4$, $\rho_{calc} = 1.469$ mg m^{-3}, $\mu = 1.970$ mm^{-1}, $F(000) = 928$, crystal size $0.12\times0.08\times0.05$ mm, θ range $= 3.29$–$79.88°$, reflections collected/unique $= 134524/16318$, ($R_{int} = 0.0617$), 1132 parameters, 120 restraints, Flack *x* parameter $= 0.091(17)$, $S = 1.096$, $R1[I > 2\sigma(I)] = 0.0572$, $wR2 = 0.1691$, $\Delta\rho_{max}$, $\Delta\rho_{min} = 0.72$, -0.28 eÅ^{-3}.

Crystal data for **5a** (CCDC 2126178): $C_{16}H_{18}F_3N_3O_2S$, $M_r = 373.39$, $T = 100(2)$ K, $\lambda = 1.54178$ Å, triclinic, space group *P*-1, $a = 5.6943(8)$, $b = 10.1985(13)$, $c = 14.0461(18)$ Å, $\alpha = 97.388(6)$, $\beta = 91.269(6)$, $\gamma = 90.090(6)°$, $V = 808.73(19)$ Å^3, $Z = 2$, $\rho_{calc} = 1.533$ mg m^{-3}, $\mu = 2.236$ mm^{-1}, $F(000) = 388$, crystal size $0.60\times0.02\times0.02$ mm, θ range $= 3.17$–$77.41°$, reflections collected/unique $= 37652/3347$, ($R_{int} = 0.0418$), 238 parameters, 45 restraints, $S = 1.058$, $R1[I > 2\sigma(I)] = 0.0685$, $wR2 = 0.2069$, $\Delta\rho_{max}$, $\Delta\rho_{min} = 1.01$, -0.37 eÅ^{-3}.

Crystal data for **7b** (CCDC 2126179): $C_{18}H_{18}F_3N_3O_5S$, $M_r = 445.41$, $T = 100(2)$ K, $\lambda = 1.54178$ Å, triclinic, space group *P*1, $a = 6.3523(7)$, $b = 9.8015(11)$, $c = 15.5546(18)$ Å, $\alpha = 83.740(4)$, $\beta = 78.303(3)$, $\gamma = 84.947(3)°$, $V = 940.53(18)$ Å^3, $Z = 2$, $\rho_{calc} = 1.573$ mg m^{-3}, $\mu = 2.155$ mm^{-1}, $F(000) = 460$, crystal size $0.14\times0.05\times0.03$ mm, θ range $= 2.91$–$80.95°$, reflections collected/unique $= 85037/7780$, ($R_{int} = 0.042$), 546 parameters, 3 restraints, Flack *x* parameter $= 0.082(17)$, $S = 1.058$, $R1[I > 2\sigma(I)] = 0.0293$, $wR2 = 0.0793$, $\Delta\rho_{max}$, $\Delta\rho_{min} = 0.21$, -0.33 eÅ^{-3}.

Crystal data for **10a** (CCDC 2126180): $C_{14}H_{14}F_3N_3O_2S$, $M_r = 345.34$, $T = 100(2)$ K, $\lambda = 0.71073$ Å, monoclinic, space group $P2_1/n$, $a = 13.1787(14)$, $b = 4.3790(5)$, $c = 25.355(3)$ Å, $\beta = 99.312(8)$, $V = 1443.9(3)$ Å^3, $Z = 4$, $\rho_{calc} = 1.589$ mg m^{-3}, $\mu = 0.271$ mm^{-1}, $F(000) = 712$, crystal size $0.12\times0.11\times0.07$ mm, θ range $= 2.68$–$35.06°$, reflections collected/unique $= 32929/6369$, ($R_{int} = 0.0700$), 208 parameters, $S = 1.021$, $R1[I > 2\sigma(I)] = 0.0461$, $wR2 = 0.1211$, $\Delta\rho_{max}$, $\Delta\rho_{min} = 0.59$, -0.75 eÅ^{-3}.

Acknowledgements

We would like to thank Professor Christian W. Lehmann for providing access to the X-ray diffraction facility at the Max-Planck-Institut für Kohlenforschung (Mülheim an der Ruhr, Germany), Heike Schucht and Elke Dreher for technical assistance with the X-ray intensity data collections, and Dr. Christian Ihling and Antje Herbrich-Peters for recording the HRMS and UV/Vis spectra. Thanks are due to Dr. Jens-Ulrich Rahfeld and Dr. Nadine Taudte for providing and maintaining the biosafety level 2 laboratory. A. R. would like to thank Professor Yossef Av-Gay for his support. Open Access funding enabled and organized by Projekt DEAL.

Conflict of Interest

The authors declare no conflict of interest.

Data Availability Statement

The data that support the findings of this study are available in the supplementary material of this article.

Keywords: benzothiazinones · BTZ043 · benzothiazines · DprE1 inhibitors · tuberculosis

[1] a) V. Makarov, G. Manina, K. Mikusova, U. Möllmann, O. Ryabova, B. Saint-Joanis, N. Dhar, M. R. Pasca, S. Buroni, A. P. Lucarelli, A. Milano, E. De Rossi, M. Belanova, A. Bobovska, P. Dianiskova, J. Kordulakova, C. Sala, E. Fullam, P. Schneider, J. D. McKinney, P. Brodin, T. Christophe, S. Waddell, P. Butcher, J. Albrethsen, I. Rosenkrands, R. Brosch, V. Nandi, S. Bharath, S. Gaonkar, R. K. Shandil, V. Balasubramanian, T. Balganesh, S. Tyagi, J. Grosset, G. Riccardi, S. T. Cole, *Science* **2009**, *324*, 801–804; b) I. Rudolph, P. Imming, A. Richter, *DE102014012546*, Martin-Luther-Universitaet Halle-Wittenberg, Germany, **2014**.
[2] V. Makarov, K. Mikušová, *Appl. Sci.* **2020**, *10*, 2269.
[3] a) G. S. Shetye, S. G. Franzblau, S. Cho, *Transl. Res.* **2020**, *220*, 68–97; b) A. Chauhan, M. Kumar, A. Kumar, K. Kanchan, *Life Sci.* **2021**, *274*, 119301.
[4] R. Tiwari, G. C. Moraski, V. Krchňák, P. A. Miller, M. Colon-Martinez, E. Herrero, A. G. Oliver, M. J. Miller, *J. Am. Chem. Soc.* **2013**, *135*, 3539–3549.
[5] A. Richter, I. Rudolph, U. Möllmann, K. Voigt, C.-W. Chung, O. M. P. Singh, M. Rees, A. Mendoza-Losana, R. Bates, L. Ballell, S. Batt, N. Veerapen, K. Fütterer, G. Besra, P. Imming, A. Argyrou, *Sci. Rep.* **2018**, *8*, 13473.
[6] T. Eckhardt, R. Goddard, C. Lehmann, A. Richter, H. A. Sahile, R. Liu, R. Tiwari, A. G. Oliver, M. J. Miller, R. W. Seidel, P. Imming, *Acta Crystallogr. Sect. C* **2020**, *76*, 907–913.
[7] R. Tiwari, P. A. Miller, S. Cho, S. G. Franzblau, M. J. Miller, *ACS Med. Chem. Lett.* **2015**, *6*, 128–133.
[8] F. Kloss, V. Krchnak, A. Krchnakova, S. Schieferdecker, J. Dreisbach, V. Krone, U. Möllmann, M. Hoelscher, M. J. Miller, *Angew. Chem. Int. Ed.* **2017**, *56*, 2187–2191; *Angew. Chem.* **2017**, *129*, 2220–2225.
[9] R. Liu, L. Markley, P. A. Miller, S. Franzblau, G. Shetye, R. Ma, K. Savková, K. Mikušová, B. S. Lee, K. Pethe, G. C. Moraski, M. J. Miller, *RSC Med. Chem.* **2021**, *12*, 62–72.
[10] a) G. Zhang, M. Howe, C. C. Aldrich, *ACS Med. Chem. Lett.* **2019**, *10*, 348–351; b) G. Zhang, L. Sheng, P. Hegde, Y. Li, C. C. Aldrich, *Med. Chem. Res.* **2021**, *30*, 449–458; c) L. Liu, C. Kong, M. Fumagalli, K. Savková, Y. Xu, S. Huszár, J. C. Sammartino, D. Fan, L. R. Chiarelli, K. Mikušová, Z. Sun, C. Qiao, *Eur. J. Med. Chem.* **2020**, *208*, 112773.
[11] A. Patel, N. Redinger, A. Richter, A. Woods, P. R. Neumann, G. Keegan, N. Childerhouse, P. Imming, U. E. Schaible, B. Forbes, L. A. Dailey, *J. Controlled Release* **2020**, *328*, 339–349.
[12] C. R. Groom, I. J. Bruno, M. P. Lightfoot, S. C. Ward, *Acta Crystallogr. Sect. B* **2016**, *72*, 171–179.
[13] F. H. Allen, D. G. Watson, L. Brammer, A. G. Orpen, R. Taylor, in *International Tables for Crystallography Volume C: Mathematical, physical and chemical tables* (Ed.: E. Prince), Springer Netherlands, Dordrecht, **2004**, pp. 790–811.
[14] K. M. Steed, J. W. Steed, *Chem. Rev.* **2015**, *115*, 2895–2933.
[15] A. L. Spek, *Acta Crystallogr. Sect. D* **2009**, *65*, 148–155.
[16] H. Flack, *Acta Crystallogr. Sect. A* **1983**, *39*, 876–881.
[17] A. Richter, M. Patzer, R. Goddard, J. B. Lingnau, P. Imming, R. W. Seidel, *J. Mol. Struct.* **2022**, *1248*, 131419.
[18] T. J. A. Sundarsingh, J. Ranjitha, A. Rajan, V. Shankar, *J. Infect. Public Health* **2020**, *13*, 1255–1264.
[19] F. Kloss, S. Schieferdecker, A. Brakhage, J. Dreisbach, M. J. Miller, U. Moellmann, K. P. Wojtas, *WO 2018/055048 Al*, Leibniz-Institut fuer Naturstoff-Forschung und Infektionsbiologie e.V. Hans-Knoell Institut HKI, Germany, **2018**.
[20] V. Makarov, B. Lechartier, M. Zhang, J. Neres, A. M. van der Sar, S. A. Raadsen, R. C. Hartkoorn, O. B. Ryabova, A. Vocat, L. A. Decosterd, N. Widmer, T. Buclin, W. Bitter, K. Andries, F. Pojer, P. J. Dyson, S. T. Cole, *EMBO Mol. Med.* **2014**, *6*, 372–383.
[21] a) A. L. Whiting, K. I. Dubicki, F. Hof, *Eur. J. Org. Chem.* **2013**, *2013*, 6802–6810; b) J. P. Powers, S. Li, J. C. Jaen, J. Liu, N. P. C. Walker, Z. Wang, H. Wesche, *Bioorg. Med. Chem. Lett.* **2006**, *16*, 2842–2845.
[22] a) R. Sathunuru, H. Zhang, C. W. Rees, E. Biehl, *Heterocycles* **2005**, *65*, 1615–1628; b) N. C. Sandhya, Chandra, G. P. Suresha, N. K. Lokanath, M. Mahendra, *Acta Crystallogr. Sect. E* **2015**, *71*, o74.
[23] a) R. Tiwari, P. A. Miller, L. R. Chiarelli, G. Mori, M. Šarkan, I. Centárová, S. Cho, K. Mikušová, S. G. Franzblau, A. G. Oliver, M. J. Miller, *ACS Med. Chem. Lett.* **2016**, *7*, 266–270; b) C. Trefzer, H. Škovierová, S. Buroni, A. Bobovská, S. Nenci, E. Molteni, F. Pojer, M. R. Pasca, V. Makarov, S. T. Cole, G. Riccardi, K. Mikušová, K. Johnsson, *J. Am. Chem. Soc.* **2012**, *134*, 912–915; c) C. Trefzer, M. Rengifo-Gonzalez, M. J. Hinner, P. Schneider, V. Makarov, S. T. Cole, K. Johnsson, *J. Am. Chem. Soc.* **2010**, *132*, 13663–13665; d) J. Neres, F. Pojer, E. Molteni, L. R. Chiarelli, N. Dhar, S. Boy-Röttger, S. Buroni, E. Fullam, G. Degiacomi, A. P. Lucarelli, R. J. Read, G. Zanoni, D. E. Edmondson, E. De Rossi, M. R. Pasca, J. D. McKinney, P. J. Dyson, G. Riccardi, A. Mattevi, S. T. Cole, C. Binda, *Sci. Transl. Med.* **2012**, *4*, 150ra121.

Manuscript received: January 11, 2022
Version of record online: February 15, 2022